

# What is the Mechanism of $H_3^+$ Formation from Cyclopropane?

Sung Kwon, Shawn Sandhu, Moaid Shaik, Jacob Stamm, Jesse Sandhu, Rituparna Das, Caitlin V. Hetherington, Benjamin G. Levine, and Marcos Dantus\*

Cite This: *J. Phys. Chem. A* 2023, 127, 8633–8638

Read Online

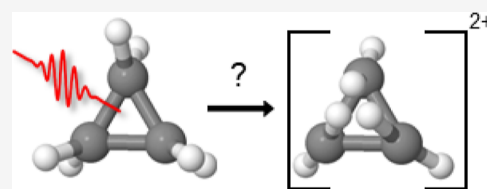
ACCESS |

Metrics & More

Article Recommendations

Supporting Information

**ABSTRACT:** We examine the possibility that three hydrogen atoms in one plane of the cyclopropane dication come together in a concerted “ring-closing” mechanism to form  $H_3^+$ , a crucial cation in interstellar gas-phase chemistry. Ultrafast strong-field ionization followed by disruptive probing measurements indicates that the formation time of  $H_3^+$  is  $249 \pm 16$  fs. This time scale is not consistent with a concerted mechanism, but rather a process that is preceded by ring opening. Measurements on propene, an isomer of cyclopropane, reveal the  $H_3^+$  formation time to be  $225 \pm 13$  fs, a time scale similar to the  $H_3^+$  formation time in cyclopropane. Ab initio molecular dynamics simulations and the fact that both dications share a common potential energy surface support the ring-opening mechanism. The reaction mechanism following double ionization of cyclopropane involves ring opening, then H-migration, and roaming of a neutral  $H_2$  molecule, which then abstracts a proton to form  $H_3^+$ . These results further our understanding of complex interstellar chemical reactions and gas-phase reaction dynamics relevant to electron ionization mass spectrometry.



## 1. INTRODUCTION

Our interest in  $H_3^+$  forming reactions is related to astrochemistry.  $H_3^+$  acts as an interstellar acid in a proton-hop reaction and promotes the formation of water and other small molecules in interstellar space, crucial molecules to initiate star formation.<sup>1,2</sup> The gas-phase reactivity of this compound is enhanced by the fact that it is triatomic, leaving a third body to carry away the excess energy. As  $H_3^+$  is one of the most abundant triatomic cations in the universe, it is important to understand its formation from various organic molecules upon double ionization because of similarities to its formation as a result of  $H_2 + H_2^+$  collisions.<sup>3,4</sup> Furthermore, small organic molecules have been found to be a minor, but additional source of  $H_3^+$  in the interstellar medium.<sup>5</sup>

Ultrafast dissociative ionization methods allow researchers to explore the mechanism of formation of fragment ions, including  $H_3^+$ , by irradiating molecules with powerful femto-second laser pulses.<sup>6–8</sup> It must be noted that the unimolecular reaction that leads to  $H_3^+$  formation requires the breaking of three bonds and formation of three new H–H bonds, which often involves significant deformation of the molecular geometry. Therefore, studying the mechanism of  $H_3^+$  formation from ionized hydrocarbons deepens our understanding of such complex ultrafast molecular dynamics and inspires approaches to control them.<sup>9–12</sup>

$H_3^+$  has been observed from the fragmentation of doubly ionized molecules.<sup>7,8,13–16</sup> The  $H_3^+$  formation reaction in ethane involves hydrogen migration, and theory indicates a transition state in which  $H_2$  is attached to the remaining dication.<sup>14,15</sup> Another mechanism, known as roaming, is observed in alcohols and other small organic molecules. In this mechanism, upon double ionization, two hydrogen atoms

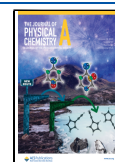
combine to form  $H_2$  which then undergoes roaming in proximity to the dication before eventually abstracting a proton to form.<sup>7,8,17–19</sup>

The dissociative double photoionization of cyclopropane has been examined previously in the 25–35 eV photon range.<sup>20</sup> In that study, which included ab initio calculations at the level CASSCF/CASPT2 theory and cc-pVTZ basis-set, the double ionization potential was calculated to be 31.28 eV, and the appearance energy for the following doubly charged species was determined to be  $C_3H_2^{2+}$  (34.0 eV),  $C_3H_3^{2+}$  (35.0 eV),  $C_3H_4^{2+}$  (30.5 eV), and  $C_3H_5^{2+}$  (33.0 eV). It was found that several dissociation channels appeared below the double ionization potential, indicating that Jahn–Teller distortion led to symmetry breaking. The extent of ring deformation and H-evaporation populates different dication states, which act as gateway states for different dissociation channels. Ring opening was associated with  $C_3H_4^{2+}$  and ring closing was associated with  $C_3H_5^{2+}$ . Furthermore, Oghbaie et al. proposed a novel ring-closing mechanism for the formation of  $H_3^+$  that preserves the  $D_{3h}$  symmetry upon double ionization and involves the simultaneous dissociation of three C–H bonds,<sup>20</sup> as shown in Figure 1. We were intrigued by their proposal of a new  $H_3^+$  formation mechanism and embarked on the present study.

Received: August 11, 2023

Revised: September 21, 2023

Published: October 9, 2023



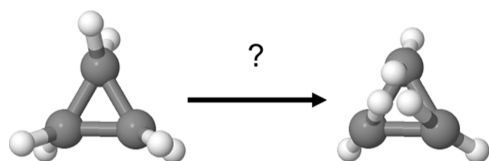


**Figure 1.** Proposed ring-closing mechanism, where three hydrogens come together on the same plane of doubly ionized cyclopropane. Jmol software was used to make this figure.<sup>21</sup>

## 2. METHODS

The experimental methodology used here to track multiple reaction pathways following ultrafast ionization, has been described in detail elsewhere.<sup>22</sup> In short, a Ti:sapphire laser producing 35 fs pulses with a central wavelength of 800 nm was used as the ionization source. The pulses were compressed using the multiphoton intrapulse interference phase scan method,<sup>23</sup> which measures and compresses the pulses using a pulse shaper. The laser pulses were focused inside a Wiley–McLaren time-of-flight (TOF) mass spectrometer via a concave gold-coated mirror. Each pulse was split into a strong pump ( $5.5 \times 10^{14}$  W/cm<sup>2</sup>), which causes tunnel ionization, and a weak probe ( $9.5 \times 10^{13}$  W/cm<sup>2</sup>), which disrupts product formation. The laser intensities were calibrated by measuring the ratio between Ar<sup>+</sup> and Ar<sup>2+</sup> ions.<sup>24</sup>

Given the ionization potentials of cyclopropane and propene (9.90 and 9.73 eV, respectively),<sup>25</sup> the intensity of the pump yielded Keldysh parameters of 0.39 for both compounds,<sup>26</sup> indicating that ionization occurs within an optical cycle via tunnel ionization. The cyclopropane and propene gases were introduced to the TOF chamber via an effusive beam through a needle valve. The static pressure inside the vacuum chamber during data acquisition was maintained at  $7 \times 10^{-6}$  Torr. The baseline vacuum pressure was  $9 \times 10^{-8}$  Torr, and when the needle valve was closed, the pressure returned to baseline within seconds, ensuring fast sample refresh. The ion signals were digitized using an oscilloscope (LeCroy WaveRunner 610Zi, 1 GHz). For H<sub>3</sub><sup>+</sup> time-resolved data, a  $-125$  V bias in the X direction was applied by using a pair of plates located before the field-free region of the TOF to avoid saturation of peaks with relatively large  $m/z$  ratios. The TOF was configured to measure positive ions, therefore, only cationic peaks are shown in the mass spectra.

To gain further insight into the mechanistic details of H<sub>3</sub><sup>+</sup> formation in cyclopropane, we conducted ab initio molecular dynamics (AIMD) using the GPU-accelerated electronic structure package TeraChem.<sup>27–29</sup> All trajectories were carried out using B3LYP/aug-cc-pVDZ with a velocity Verlet integrator with a time step of 0.5 fs and integrated for up to 750 fs. A total of 500 trajectories were computed for each molecule. For all trajectories, the initial position and momentum were sampled from the neutral ground state Wigner distribution using the aforementioned level of theory. Trajectories were initiated on the dication ground state potential energy surface (PES), assuming vertical excitation of the neutral. All trajectories and molecular geometries were visualized using Avogadro.<sup>30,31</sup> Using TeraChem, the geometries (both minima and transition states) for the potential energy curve were calculated using B3LYP/aug-cc-pVDZ. The single-point energies were determined using CCSD(T)/aug-cc-pVDZ implemented in GAMESS.<sup>32–34</sup> We found good agreement (differences <0.25 eV) between the energies calculated by both methods.

## 3. RESULTS AND DISCUSSION

The experimental strong-field ionization (SFI) mass spectra of cyclopropane and propene are shown in Figure 2. We found

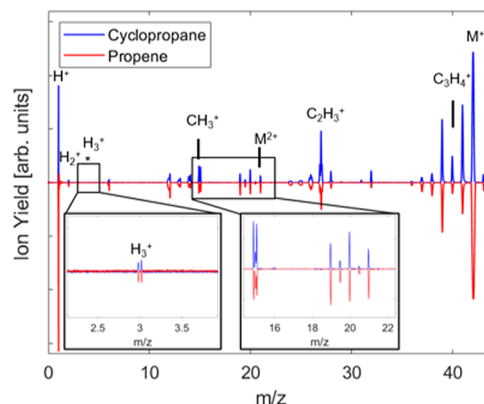


**Figure 2.** SFI mass spectra of cyclopropane (blue) and propene (red). The single pulse intensity for ionization was  $5.5 \times 10^{14}$  W/cm<sup>2</sup>. Each spectrum was normalized by dividing the amplitude by the sum of all peak areas. The left inset shows a zoomed-in region of the spectra where the H<sub>3</sub><sup>+</sup> is observed. The inset on the right shows the CH<sub>3</sub><sup>+</sup> and C<sub>3</sub>H<sub>4</sub><sup>+</sup> fragments.

both SFI spectra to be very similar. The peak at  $m/z$  15 corresponds to CH<sub>3</sub><sup>+</sup> in both compounds, which suggests that hydrogen migration occurs in cyclopropane. In fact, the CH<sub>3</sub><sup>+</sup> yield is greater for cyclopropane. In addition, we observe that for the dication fragments, loss of two hydrogens occurs with greater probability than loss of individual hydrogen atoms. This likely implies that loss of neutral H<sub>2</sub> from both compounds is favored over loss of individual hydrogen atoms.

We compare the SFI spectrum obtained with that obtained by Oghbaie et al.<sup>20</sup> to ensure similar internal energies, allowing us to evaluate if the formation of H<sub>3</sub><sup>+</sup> follows their suggested ring-closing mechanism. This determination is done by matching the abundance of “thermometer ions”.<sup>35</sup> The SFI spectrum of cyclopropane is in very close agreement with the single 35 eV photoionization of cyclopropane, as determined by the similar relative ion yields for all  $m/z$  values.<sup>20</sup> This indicates that the SFI process leads to a vertical ionization energy similar to that of the 35 eV photoionization. Further evidence of the internal energy acquired by the molecules during SFI comes from the observation of H<sub>3</sub><sup>+</sup> and C<sub>3</sub>H<sub>3</sub><sup>2+</sup>, which have appearance energies of 32.5 and 35.0 eV, respectively.<sup>20</sup>

The H<sub>3</sub><sup>+</sup> ion appears as a doublet in the TOF spectrum as a result of the Coulomb repulsion between H<sub>3</sub><sup>+</sup> and the counterion. The forward and backward ejections along the TOF lead to different times of arrival, which can be used to determine the kinetic energy release (KER) of this fragment (Figure S1). The H<sub>3</sub><sup>+</sup> doublet was integrated as a function of the delay between the pump and probe pulses. The time-resolved dynamics of H<sub>3</sub><sup>+</sup> from cyclopropane and propene is shown in Figure 3. The positive feature at zero delay between pump and probe pulses is caused by the increased intensity of the time-overlapped pulses, which causes a greater ion yield as their intensities sum when overlapped in time. The depletion that follows is caused by the probe pulse disrupting the formation of H<sub>3</sub><sup>+</sup> by shifting the branching ratio to a different reaction pathway. By tracking the decay and recovery, we can determine the time scale of formation for all ions in the mass

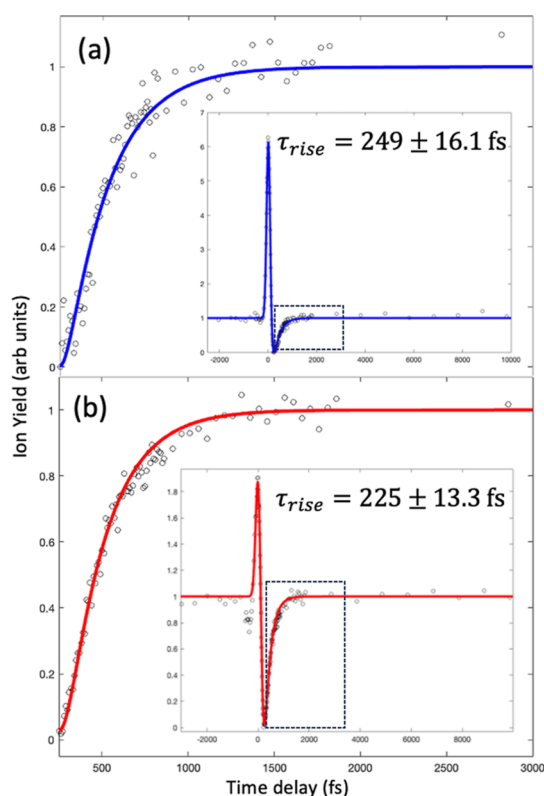


**Figure 3.** Time-resolved fitted  $\text{H}_3^+$  ion formation from (a) cyclopropane and (b) propene based on the pump–probe delay is shown in figure. The circles correspond to experimental data. The blue and red lines indicate the exponential fit corresponding to eq 2.

spectrum, including  $\text{H}_3^+$ . The entire experimental transient can be fit to the function

$$P(t, \tau_1, \tau_2) = ae^{-t^2/s^2} + bP_1(t, \tau_1) + cP_2(t, \tau_2) \quad (1)$$

where

$$P_i(t, \tau_i) = e^{-t/\tau_i} \left( 1 + \operatorname{erf} \left( \frac{t}{s} - \frac{s}{2\tau_i} \right) \right) \quad (2)$$

For the abovementioned equation,  $a$ ,  $b$ , and  $c$  are the amplitude factors,  $\tau_i$  is a time constant defining a decay ( $\tau_{\text{decay}}$ ) or rise ( $\tau_{\text{rise}}$ ) of the signal,  $t$  is a specific pump–probe delay, and  $s$  is a parameter related to the full width at half max (fwhm) of the pulse duration by

$$\tau_{\text{FWHM}} = 2\sqrt{\ln 2} \cdot s \quad (3)$$

The specific fitting parameters used can be found in the Supporting Information.

The time scale of formation of  $\text{H}_3^+$  is obtained by fitting the experimental data using eq 2 and are found to be  $\tau = 249 \pm 16$  fs and  $\tau = 225 \pm 13$  fs for cyclopropane and propene, respectively.

To gain insight into the reaction mechanism, we performed AIMD trajectories on the dication states of cyclopropane and propene. In Figure 4, we show a representative trajectory for cyclopropane where ring-opening occurs within the first 29 fs. This is followed by H migration, the formation of neutral  $\text{H}_2$ , which roams near the dication, and finally the abstraction of a proton to form  $\text{H}_3^+$  (see Video S1).

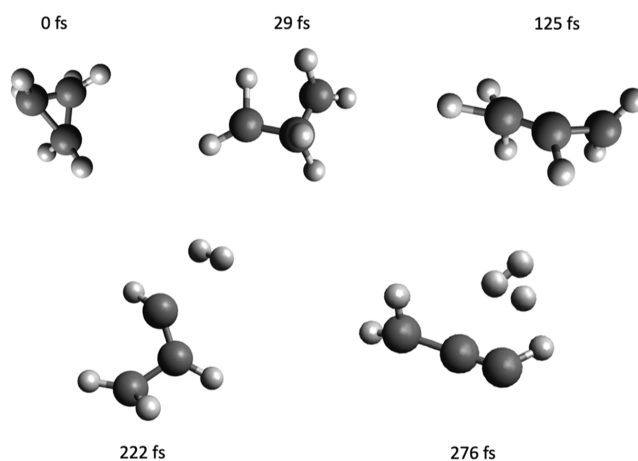


**Figure 4.** AIMD trajectory of  $\text{H}_3^+$  formation via hydrogen migration and  $\text{H}_2$  roaming. Snapshots were taken from the cyclopropane trajectory shown in Video S1. The trajectory was calculated by using B3LYP/aug-cc-pVDZ.

We find that some reaction pathways that lead to the formation of  $\text{H}_3^+$  for both molecules share the same intermediates and transition states (Figure 5 and Video S1). For both molecules, the dication minimum is identical (Figure 5) with equal positive charge densities on both carbon ends (Figure S2). From 500 AIMD trajectories for each compound, 10 and 9 trajectories for cyclopropane and propene, respectively, resulted in  $\text{H}_3^+$  formation. All 500 trajectories for cyclopropane showed ring opening occurring within 30 fs of double ionization. The average time scale of the trajectories forming  $\text{H}_3^+$  was 281 and 271 fs for cyclopropane and propene, respectively. These values are in close agreement with our experimental measurements.

The similarities in  $\text{H}_3^+$  formation time scales support the ring-opening mechanism in cyclopropane. Moreover, these time scales show that the slightly longer  $\text{H}_3^+$  formation time for cyclopropane is partially due to the time for ring opening.

We find the relatively long time scale of the  $\text{H}_3^+$  formation and the AIMD trajectories to be inconsistent with the ring-closing mechanism proposed by Oghbaie et al.<sup>20</sup> One would expect the ring-closing mechanism, which involves the concerted coalescence of three hydrogen atoms on the same plane of cyclopropane, to occur in a single kinetic step on a time scale of a few hydrogen-puckering vibrational periods (the symmetric  $\nu_3$  mode,  $851 \text{ cm}^{-1}$ , B3LYP/aug-cc-pVDZ,  $\sim 39$  fs period). Thus, we propose that the dominant mechanism of  $\text{H}_3^+$  formation is the ring-opening mechanism. This is additionally supported by the SFI spectrum, as well as the photoionization spectrum,<sup>20</sup> which show a 4–6 times greater yield for  $\text{C}_3\text{H}_4^{2+}$  fragment (associated with ring opening) than  $\text{C}_3\text{H}_5^{2+}$  fragment (associated with ring closing). Also, the similarity found in the KER analysis of the  $\text{H}_3^+$  peaks for both compounds provides further evidence for the ring-opening mechanism (Figure S1).

Having identified the ring-opening mechanism identified, high-level quantum chemical calculations were used to quantify the associated energetics. Several intermediate structures common to cyclopropane and propene are observed prior to the formation of  $\text{H}_3^+$  as seen in Figure 5. We found that the density functional theory PES used in the AIMD trajectories is in very good agreement with the energies computed at the CCSD(T) level (Figure 5). The positive charges on both

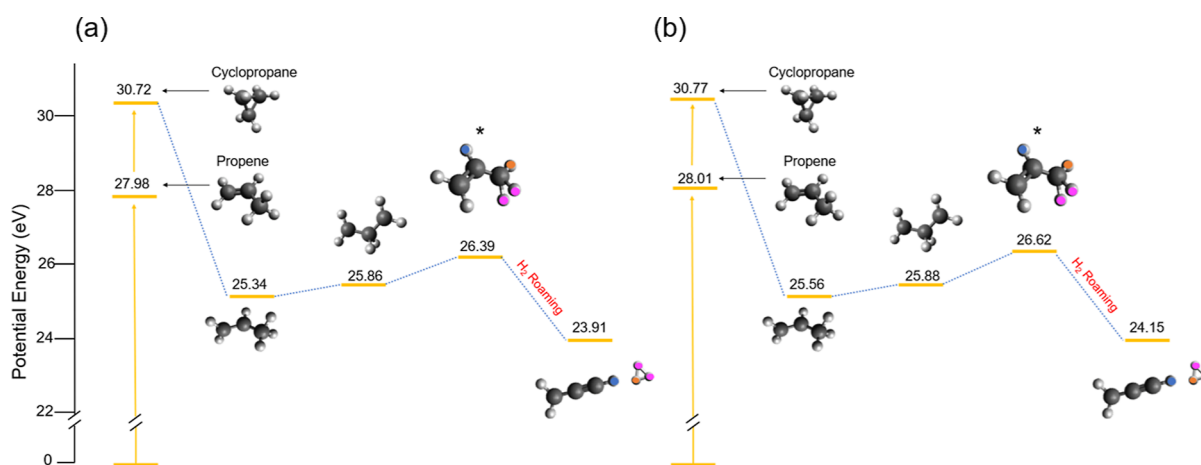


**Figure 5.** Potential energy diagram for cyclopropane and propene depicting the formation of  $\text{H}_3^+$ . The geometries were optimized using B3LYP/aug-cc-pVDZ, and the energies were calculated for (a) using CCSD(T)/aug-cc-pVDZ and for (b) using B3LYP/aug-cc-pVDZ. Transition states are denoted by asterisks next to the structure. Initially, one hydrogen atom migrates from the middle carbon (colored orange) to join the two other hydrogen atoms on a terminal carbon (colored pink); this step is followed by formation of neutral  $\text{H}_2$ , and upon proton abstraction, the remaining H atom (colored blue) in the central carbon migrates to the end carbon.

carbon ends pull electron density away from the secondary carbon, weakening its C–H bonds (Figure S2). This is a key step prior to hydrogen migration and formation of  $\text{H}_2$ . The excess energy following double ionization provides the driving force, which allows for bond cleavage and rearrangements.

In all observed trajectories in which  $\text{H}_3^+$  was formed, we noticed that after hydrogen migration, neutral  $\text{H}_2$  roamed near the dication before abstracting a proton (see supplementary Video S1 for a representative trajectory of  $\text{H}_3^+$  formation from cyclopropane and propene). Overall, our experimental and theoretical work provides compelling evidence that ring-opening occurs after the double ionization of cyclopropane. It remains to be explored if SFI with a laser pulse duration shorter than the 20 fs associated with Jahn–Teller distortion can cause ultrafast excitation to a different electronic state of the dication that will result in the ring-closing mechanism of  $\text{H}_3^+$  formation.

## 4. CONCLUSIONS

We determined the dominant mechanism of  $\text{H}_3^+$  formation from doubly ionized cyclopropane to be ring opening, followed by hydrogen migration, formation of neutral  $\text{H}_2$ , roaming, and proton abstraction to form  $\text{H}_3^+$ . This conclusion is supported by experimental ultrafast dynamics, ab initio molecular dynamics, and ab initio electronic structure calculations. The experimental  $\text{H}_3^+$  formation time scale from cyclopropane is 249 fs and provides compelling evidence for the proposed ring-opening mechanism, rather than the ring-closing mechanism previously suggested in the literature. Furthermore, doubly ionized propene was observed to form  $\text{H}_3^+$  in 225 fs, a time scale close to the formation of  $\text{H}_3^+$  from cyclopropane. The findings presented in this study contribute to our understanding of gas-phase chemistry and complex dynamics following the ionization of organic molecules leading to  $\text{H}_3^+$ .

## ■ ASSOCIATED CONTENT

### Supporting Information

The Supporting Information is available free of charge at <https://pubs.acs.org/doi/10.1021/acs.jpca.3c05442>.

AIMD trajectories showing H migration, the formation of neutral  $\text{H}_2$ , and the abstraction of a proton to form  $\text{H}_3^+$  for both cyclopropane and propene (MP4)

Reagents, fitting equation parameters, experimental analysis including kinetic energy release, and theoretical analysis including the Mulliken charges for the common dication minimum for cyclopropane and propene (PDF)

## ■ AUTHOR INFORMATION

### Corresponding Author

Marcos Dantus – Department of Chemistry and Department of Physics and Astronomy, Michigan State University, East Lansing, Michigan 48824, United States; [orcid.org/0000-0003-4151-5441](https://orcid.org/0000-0003-4151-5441); Email: [dantus@chemistry.msu.edu](mailto:dantus@chemistry.msu.edu)

### Authors

Sung Kwon – Department of Chemistry, Michigan State University, East Lansing, Michigan 48824, United States  
 Shawn Sandhu – Department of Chemistry, Michigan State University, East Lansing, Michigan 48824, United States; [orcid.org/0000-0001-6252-4270](https://orcid.org/0000-0001-6252-4270)  
 Moaid Shaik – Department of Chemistry, Michigan State University, East Lansing, Michigan 48824, United States  
 Jacob Stamm – Department of Chemistry, Michigan State University, East Lansing, Michigan 48824, United States  
 Jesse Sandhu – Department of Chemistry, Michigan State University, East Lansing, Michigan 48824, United States  
 Rituparna Das – Department of Chemistry, Michigan State University, East Lansing, Michigan 48824, United States  
 Caitlin V. Hetherington – Department of Chemistry and Institute of Advanced Computational Science, Stony Brook University, Stony Brook, New York 11794, United States; [orcid.org/0000-0003-1839-2500](https://orcid.org/0000-0003-1839-2500)  
 Benjamin G. Levine – Department of Chemistry and Institute of Advanced Computational Science, Stony Brook University, Stony Brook, New York 11794, United States; [orcid.org/0000-0002-0356-0738](https://orcid.org/0000-0002-0356-0738)

Complete contact information is available at: <https://pubs.acs.org/doi/10.1021/acs.jpca.3c05442>



## Notes

The authors declare no competing financial interest.

## ACKNOWLEDGMENTS

This material is based on the work supported by the Department of Energy, Office of Basic Energy Sciences, Atomic, Molecular, and Optical Sciences Program under award number SISGR (DE-SC0002325). R.D. was funded by the Air Force Office of Scientific Research under award number FA9550-21-1-0428. This work used the SDSC Expanse GPU at San Diego Supercomputer Center through allocation CHE230046 from the Advanced Cyberinfrastructure Coordination Ecosystem: Services & Support (ACCESS) program, which is supported by National Science Foundation grants #2138259, #2138286, #2138307, #2137603, and #2138296. B.G.L. gratefully acknowledges support from the National Science Foundation CHE-1954519.

## REFERENCES

- (1) Watson, W. D. The rate of formation of interstellar molecules by ion–molecule reactions. *Astrophys. J.* **1973**, *183*, L17.
- (2) Oka, T. Interstellar H<sup>3+</sup>. *Chem. Rev.* **2013**, *113*, 8738–8761.
- (3) Zhou, L.; Ni, H.; Jiang, Z.; Qiang, J.; Jiang, W.; Zhang, W.; Lu, P.; Wen, J.; Lin, K.; Zhu, M.; et al. Ultrafast formation dynamics of D<sup>3+</sup> from the light-driven bimolecular reaction of the D<sub>2</sub>–D<sub>2</sub> dimer. *Nat. Chem.* **2023**, *15*, 1229–1235.
- (4) Mi, Y.; Wang, E.; Dube, Z.; Wang, T.; Naumov, A.; Villeneuve, D.; Corkum, P.; Staudte, A. D<sup>3+</sup> formation through photoionization of the molecular D<sub>2</sub>-D<sub>2</sub> dimer. *Nat. Chem.* **2023**, *15*, 1224–1228.
- (5) Pilling, S.; Andrade, D.; Neves, R.; Ferreira-Rodrigues, A.; Santos, A.; Boechat-Roberty, H. Production of H<sup>3+</sup> via photodissociation of organic molecules in interstellar clouds: H<sup>3+</sup> photoproduction in interstellar clouds. *Mon. Not. R. Astron. Soc.* **2007**, *375*, 1488–1494.
- (6) Kotsina, N.; Kaziannis, S.; Kosmidis, C. Hydrogen migration in methanol studied under asymmetric fs laser irradiation. *Chem. Phys. Lett.* **2014**, *604*, 27–32.
- (7) Ekanayake, N.; Nairat, M.; Kaderiya, B.; Feizollah, P.; Jochim, B.; Severt, T.; Berry, B.; Pandiri, K. R.; Carnes, K. D.; Pathak, S.; et al. Mechanisms and time-resolved dynamics for trihydrogen cation H<sup>3+</sup> formation from organic molecules in strong laser fields. *Sci. Rep.* **2017**, *7*, 4703.
- (8) Ekanayake, N.; Severt, T.; Nairat, M.; Weingartz, N. P.; Farris, B. M.; Kaderiya, B.; Feizollah, P.; Jochim, B.; Ziaee, F.; Borne, K.; et al. H<sub>2</sub> roaming chemistry and the formation of H<sup>3+</sup> from organic molecules in strong laser fields. *Nat. Commun.* **2018**, *9*, 5186.
- (9) Kaziannis, S.; Kotsina, N.; Kosmidis, C. Interaction of toluene with two-color asymmetric laser fields: Controlling the directional emission of molecular hydrogen fragments. *J. Chem. Phys.* **2014**, *141*, 104319.
- (10) Michie, M. J.; Ekanayake, N.; Weingartz, N. P.; Stamm, J.; Dantus, M. Quantum coherent control of h<sup>3+</sup> formation in strong fields. *J. Chem. Phys.* **2019**, *150*, 044303.
- (11) Iwamoto, N.; Schwartz, C. J.; Jochim, B.; Raju, P. K.; Feizollah, P.; Napierala, J.; Severt, T.; Tegegn, S.; Solomon, A.; Zhao, S.; et al. Strong-field control of H<sup>3+</sup> production from methanol dications: Selecting between local and extended formation mechanisms. *J. Chem. Phys.* **2020**, *152*, 054302.
- (12) Townsend, T.; Schwartz, C. J.; Jochim, B.; Raju, P. K.; Severt, T.; Iwamoto, N.; Napierala, J.; Feizollah, P.; Tegegn, S.; Solomon, A.; et al. Controlling H<sup>3+</sup> formation from ethane using shaped ultrafast laser pulses. *Front. Phys.* **2021**, *9*, 691727.
- (13) De, S.; Rajput, J.; Roy, A.; Ghosh, P.; Safvan, C. Formation of H<sup>3+</sup> due to intramolecular bond rearrangement in doubly charged methanol. *Phys. Rev. Lett.* **2006**, *97*, 213201.
- (14) Hoshina, K.; Furukawa, Y.; Okino, T.; Yamanouchi, K. Efficient ejection of H<sup>3+</sup> from hydrocarbon molecules induced by ultrashort intense laser fields. *J. Chem. Phys.* **2008**, *129*, 104302.
- (15) Kraus, P. M.; Schwarzer, M. C.; Schirmel, N.; Urbasch, G.; Frenking, G.; Weitzel, K.-M. Unusual mechanism for H<sup>3+</sup> formation from ethane as obtained by femtosecond laser pulse ionization and quantum chemical calculations. *J. Chem. Phys.* **2011**, *134*, 114302.
- (16) Ando, T.; Shimamoto, A.; Miura, S.; Iwasaki, A.; Nakai, K.; Yamanouchi, K. Coherent vibrations in methanol cation probed by periodic H<sup>3+</sup> ejection after double ionization. *Commun. Chem.* **2018**, *1*, 7.
- (17) Nakai, K.; Kato, T.; Kono, H.; Yamanouchi, K. Communication: Long-lived neutral H<sub>2</sub> in hydrogen migration within methanol dication. *J. Chem. Phys.* **2013**, *139*, 181103.
- (18) Livshits, E.; Luzon, I.; Gope, K.; Baer, R.; Strasser, D. Time-resolving the ultrafast H<sub>2</sub> roaming chemistry and H<sup>3+</sup> formation using extreme-ultraviolet pulses. *Nat. Comm. Chem.* **2020**, *3*, 49.
- (19) Wang, E.; Shan, X.; Chen, L.; Pfeifer, T.; Chen, X.; Ren, X.; Dorn, A. Ultrafast proton transfer dynamics on the repulsive potential of the ethanol dication: Roaming-mediated isomerization versus coulomb explosion. *J. Chem. Phys. A* **2020**, *124*, 2785–2791.
- (20) Oghbaie, S.; Gisselbrecht, M.; Månsson, E. P.; Laksman, J.; Strählman, C.; Sankari, A.; Sorensen, S. L. Dissociation of cyclopropane in double ionization continuum. *Phys. Chem. Chem. Phys.* **2017**, *19*, 19631–19639.
- (21) Jmol: an open-source java viewer for chemical structures in 3d. version 14.6.4. 2023, <http://avogadro.ccweb/> (accessed Oct 8, 2023).
- (22) Jochim, B.; DeJesus, L.; Dantus, M. Ultrafast disruptive probing: simultaneously keeping track of tens of reaction pathways. *Rev. Sci. Instrum.* **2022**, *93*, 033003.
- (23) Xu, B.; Gunn, J. M.; Cruz, J. M. D.; Lozovoy, V. V.; Dantus, M. Quantitative investigation of the multiphoton intrapulse interference phase scan method for simultaneous phase measurement and compensation of femtosecond laser pulses. *J. Opt. Soc. Am. B* **2006**, *23*, 750–759.
- (24) Guo, C.; Li, M.; Nibarger, J. P.; Gibson, G. N. Single and double ionization of diatomic molecules in strong laser fields. *Phys. Rev. A: At., Mol., Opt. Phys.* **1998**, *58*, R4271–R4274.
- (25) Traeger, J. C. A study of the allyl cation thermochemistry by photoionization mass spectrometry. *Int. J. Mass Spectrom. Ion Process.* **1984**, *58*, 259–271.
- (26) Keldysh, L. Ionization in the field of a strong electromagnetic wave. *J. Exp. Theor. Phys.* **1965**, *20*, 1307–1314.
- (27) Ufimtsev, I. S.; Martinez, T. J. Quantum chemistry on graphical processing units. 1. strategies for two-electron integral evaluation. *J. Chem. Theory Comput.* **2008**, *4*, 222–231.
- (28) Ufimtsev, I. S.; Martinez, T. J. Quantum chemistry on graphical processing units. 2. direct self-consistent-field implementation. *J. Chem. Theory Comput.* **2009**, *5*, 1004–1015.
- (29) Ufimtsev, I. S.; Martinez, T. J. Quantum chemistry on graphical processing units. 3. analytical energy gradients, geometry optimization, and first principles molecular dynamics. *J. Chem. Theory Comput.* **2009**, *5*, 2619–2628.
- (30) Avogadro: An open-source molecular builder and visualization tool. version 1.2.0. 2023, <http://avogadro.ccweb/> (accessed March 8, 2023).
- (31) Hanwell, M. D.; Curtis, D. E.; Lonie, D. C.; Vandermeersch, T.; Zurek, E.; Hutchison, G. R. Avogadro: an advanced semantic chemical editor, visualization, and analysis platform. *J. Cheminf.* **2012**, *4*, 17.
- (32) Schmidt, M. W.; Baldrige, K. K.; Boatz, J. A.; Elbert, S. T.; Gordon, M. S.; Jensen, J. H.; Koseki, S.; Matsunaga, N.; Nguyen, K. A.; Su, S.; et al. General atomic and molecular electronic structure system. *J. Comput. Chem.* **1993**, *14*, 1347–1363.
- (33) Piecuch, P.; Kucharski, S. A.; Kowalski, K.; Musiał, M. Efficient computer implementation of the renormalized coupled-cluster methods: the r-ccsd [t], r-ccsd (t), cr-ccsd [t], and cr-ccsd (t) approaches. *Comput. Phys. Commun.* **2002**, *149*, 71–96.

(34) Barca, G. M.; Bertoni, C.; Carrington, L.; Datta, D.; De Silva, N.; Deustua, J. E.; Fedorov, D. G.; Gour, J. R.; Gunina, A. O.; Guidez, E.; et al. Recent developments in the general atomic and molecular electronic structure system. *J. Chem. Phys.* **2020**, *152*, 154102.

(35) Barylyuk, K. V.; Chingin, K.; Balabin, R. M.; Zenobi, R. Fragmentation of benzylpyridinium “thermometer” ions and its effect on the accuracy of internal energy calibration. *J. Am. Chem. Soc.* **2010**, *21*, 172–177.